Identification of the *cis*-molecular neighbours of the immune checkpoint protein B7-H4 in the breast cancer cell-line SK-BR-3 by proteomic proximity labelling

JOHANNA S. REES[1], LAWRENCE C.C. CHEUNG[1], SAMIR W. HAMAIA[1], GARETH DAVIES[2], ALAN SANDERCOCK[3], KATHRYN S. LILLEY[1], NATALIE TIGUE[3] and ANTONY P. JACKSON[1]

[1]Department of Biochemistry, University of Cambridge, Cambridge CB2 1QW; [2]Oncology R&D, AstraZeneca; [3]Antibody Discovery and Protein Engineering, R&D, AstraZeneca, Cambridge, CB21 6GP, United Kingdom

Received September 11, 2019; Accepted January 2, 2020

DOI: 10.3892/ijo.2020.5037

Abstract. The immune checkpoint protein B7-H4 plays an important role in the positive as well as the negative regulation of immune T-cell responses. When expressed on cancer cells, B7-H4 inhibits T-cell activity, and numerous types of cancer cells use upregulation of B7-H4 as a survival strategy. Thus, B7-H4 is a potential target for anticancer drug therapy. Unfortunately, the cell biology of this molecule has yet to be fully elucidated. Even basic properties, such as the nature of B7-H4 interactors, are controversial. In particular, the *cis*-interactors of B7-H4 on cancer cell plasma membranes have not been investigated to date. The present study used a proteomic proximity-labelling assay to investigate the molecular neighbours of B7-H4 on the surface of the human breast cancer cells SK-BR-3. By comparison to a comprehensive proteome analysis of SK-BR-3 cells, the proximity method detected a relatively small number of low abundance plasma membrane proteins highly enriched for proteins known to modulate cell adhesion and immune recognition. It may be inferred that these molecules contribute to the immunosuppressive behaviour that is characteristic of B7-H4 on cancer cells.

Introduction

The B7 family of immunoregulatory proteins comprises several members expressed on antigen-presenting cells (APCs), T-cells and tumour cells (1). These are transmembrane glycoproteins, with one or more amino-terminal extracellular immunoglobulin domains, a single transmembrane alpha-helical domain, and a short intracellular region.

Correspondence to: Dr Johanna S. Rees or Dr Antony P. Jackson, Department of Biochemistry, University of Cambridge, Hopkins Building Tennis Court Road, Cambridge CB2 1QW, United Kingdom
E-mail: j.s.rees.99@cantab.net

Key words: specific proteomic proximity labelling assay using tyramide, proteomics, B7-H4, microenvironment, integrins, HLA class I histocompatibility antigen α chain E

B7 proteins are expressed on the surface of APCs and are considered to interact *in trans* with specific receptors on subsets of T-cells as part of the immune synapse that forms between these two types of cells. In so doing, they provide a co-signal for T-cell regulation that acts in concert with the *trans* interaction between the T-cell receptor and the antigen-MHC complex from the APC (2,3). The best characterised example is the protein B7-H1 (PD-L1), which recognises the programmed death-1 (PD-1) protein expressed on the surface of T-cells. This interaction can inhibit T-cell activity by stimulating T-cell apoptosis (4,5). By contrast, the structurally related protein B7-H4 (B7S1, VTCN1, B7x) is less well understood. The binding of B7-H4 to $CD4^+$ and $CD8^+$ T-cells inhibits their activation and proliferation (6). However, the *trans*-binding partner for B7-H4 at the T-cell plasma membrane has not yet been confirmed (7).

Although generally absent from most normal human tissues, the B7-H4 protein is often expressed on the plasma membrane of human cancer cells, and a high level of expression is correlated with poor prognosis (8). Expression of B7-H4 is particularly common in lung, ovarian, oesophageal and breast cancers (8-11), and is associated with an enhanced metastatic potential (12,13). It is believed that B7-H4 promotes tumour survival, at least in part, by attenuating the immune response of T-cells and other immune cells that infiltrate the tumour microenvironment (14,15).

There is increasing interest in the potential of antibody-based cancer therapy as a mechanism for blocking immune-inhibitory signals from the B7 proteins beyond the well-established PD-1:PD-L1 interaction (16,17). However, to realise the potential of this approach, a clearer understanding of the molecular context of the B7 microenvironment, both on the plasma membrane of the B7-expressing tumour cells and the immune cells that recognise them, is required. For example, an important unresolved question is whether the B7 proteins are uniformly distributed over the tumour cell plasma membrane, or whether they form a co-localised cluster of specific proteins. Such local *cis*-clustering is common for immunoregulatory molecules and may facilitate the formation of the immune synapse with the interacting immune cell (18). Identifying the *cis*-molecular neighbours of B7 family proteins

using new proximity proteomic technologies may provide new insights into their function. However, to the best of our knowledge, there are no reports in the literature that investigate this issue. In the present study, a proximity labelling method was used to take a snapshot of the plasma membrane proteins surrounding B7-H4 and characterise these proteins using orthogonal approaches.

Cis-interacting proteins need only interact weakly to maintain their associations on the two-dimensional surface of the plasma membrane; such low-affinity interactions may not be maintained once the cell is lysed. Furthermore, proteins assembled into more extended *cis*-clusters need not interact directly to be spatially and functionally associated (19). These characteristics make it difficult to characterise the composition of such clusters by simple proteomic analysis of immunoprecipitated proteins. As an alternative approach to the investigation and analysis of these two-dimensional clusters, our group has previously developed a specific proteomic proximity labelling assay using tyramide (SPPLAT) (20). In this method, peroxidase is targeted via a specific antibody to the plasma membrane protein of interest, and a biotin-tyramide derivative is briefly added. The peroxidase generates a biotin-tyramide free radical that covalently biotinylates proteins within a few tens of nm from the target. These proteins can then be isolated by streptavidin affinity capture and identified by mass spectrometry (MS) (19-21).

The SPPLAT method was used to investigate the molecular neighbours of the B7-H4 immune checkpoint protein on the surface of the human breast cancer cell line SK-BR-3. This cell line expresses B7-H4 on its plasma membrane, and has been extensively used as a model to understand the biochemistry, cell biology and pathophysiology of breast cancer (22). The aim of the present study was to determine whether the B7-H4 molecule, as well as regulating T-cell immune responses, may also play a role in modulating the cell-matrix interactions when expressed on cancer cells, which is likely to be important in metastatic survival.

Materials and methods

Experimental workflow. Stable isotope labelling of amino acids in culture (SILAC) SPPLAT methodology is schematically outlined in Fig. S1.

Cell culture. Human breast adenocarcinoma SK-BR-3 cells (ATCC) were grown in McCoy's medium or RPMI-1640 containing 2 mM L-glutamine and supplemented with 10% foetal bovine serum (Invitrogen; Thermo Fisher Scientific, Inc.). The medium was changed every 2-3 days. For SILAC experiments, the RPMI-1640 heavy medium contained $^{13}C_6$ labelled L-lysine and L-arginine (K_6R_6), while the light medium was RPMI-1640 containing non-labelled L-lysine and L-arginine (K_0R_0), both of which were supplemented with 10% dialyzed foetal bovine serum (all from Dundee Cell Products), 2 mM L-glutamine, 100 U/ml penicillin and 100 μg/ml streptomycin (all from Invitrogen; Thermo Fisher Scientific, Inc.).

Flow cytometry analysis. The cells were washed with PBS and were detached from tissue culture flasks by accutase (Gibco; Thermo Fisher Scientific, Inc.). Cells were incubated with LIVE/DEAD® fixable violet dead cell stain (20 min, 4˚C, Thermo Fisher Scientific, Inc.), washed with flow cytometry buffer (eBiosciences), and stained with AF647 (Thermo Fisher Scientific, Inc.)-conjugated anti-B7-H4 (MedImmune) or isotype control (clone R347, MedImmune) antibodies for 30 min at 4˚C. Cells were washed with flow cytometry buffer and fixed with 1% paraformaldehyde for 20 min at 4˚C before analysis. Compensation was performed using antibody-stained AbC beads (Invitrogen; Thermo Fisher Scientific, Inc.) and LIVE/DEAD® violet-stained ArC beads (Invitrogen; Thermo Fisher Scientific, Inc.). Flow cytometry was performed on an FACS Canto II with 405 and 633 nm lasers (BD Biosciences), with data analysis in FlowJo v10.0.6 software (Tree Star, Inc.).

Immunofluorescence. SK-BR-3 cells were spun onto coverslips pre-coated with 0.05% poly L-lysine, fixed with 4% paraformaldehyde at room temperature for 10 min, washed in PBS and incubated with anti-B7-H4-488 (MedImmune) for 1 h at room temperature. To determine all locations of B7-H4, the cells were permeabilised with 1% saponin for 30 min prior to antibody incubation and imaged at x60 magnification using an Olympus Fluoview IX81 laser scanning confocal microscope (Olympus Corporation).

Biotinylation of surface B7-H4 and neighbours. The biotin tyramide reagent was prepared as previously described (21). A total of 1 mg each of Human IgG1 anti-B7-H4 monoclonal antibody (in-house; MedImmune) and anti-B7-H1 (PD-L1) monoclonal antibody (in-house; MedImmune) were conjugated with HRP using the EZ-link activated peroxidase kit at pH 9.4 (cat. no. 31497; Thermo Fisher Scientific, Inc.) and purified by gel filtration. This resulted in ~1:1 stoichiometry. Exponentially growing SK-BR-3 cells were pelleted and washed in PBS at room temperature. Approximately $1x10^6$ live cells were incubated with end-over-end rotation for 2 h with either 20 μg/ml human anti-B7-H4-HRP, 20 μg/ml human anti-B7-H4 with 200 nM free HRP (BioRad Laboratories, Inc.), or 20 μg/ml human anti-B7-H1-HRP in 20 ml PBS with 10% BSA (Sigma-Aldrich; Merck KGaA) at 4˚C. For SILAC SPPLAT ~$5x10^8$ heavy (K_6R_6) cells were incubated with end-over-end rotation for 2 h with 20 μg/ml HRP-conjugated human anti-B7-H4 and $5x10^8$ light (K_0R_0) with 20 μg/ml human anti-B7-H4 and 200 nM free HRP.

Cells were pelleted and re-suspended in 10 ml tyramide-labelling buffer (50 mM Tris HCl pH7.4, fresh 0.03% H_2O_2 and 80 μg/μl tyramide biotin label (Thermo Fisher Scientific, Inc.) and incubated with end-over-end rotation at room temperature for 5 min. After incubation, 100 U/ml catalase (Sigma-Aldrich; Merck KGaA) was added and incubated with the samples for a further 5 min to quench H_2O_2. Cells were washed gently with 45 ml antibody strip buffer [50 mM glycine (pH 3.0), 150 mM NaCl, 0.9 mM $CaCl_2$, 0.5 mM $MgCl_2$] and left on ice for 5 min. The extent of biotinylation was assessed by immunofluorescence using non-permeabilised cells stained with Streptavidin-488 (at 1:100) for 1 h at room temperature.

Affinity purification of biotinylated proteins. Cells were re-suspended in 15 ml cell lysis buffer [20 mM Tris-HCl (pH 7.5), 5 mM EDTA, 1X protease inhibitor cocktail (Roche Diagnostics), 150 mM NaCl, 1% v/v Triton X-100,

0.1 M sodium thiocyanate (Sigma-Aldrich; Merck KGaA)] and incubated for 30 min on ice. Insoluble material was removed by centrifugation at 10,000 x g for 10 min at 4˚C, and the protein-containing soluble fraction was recovered for streptavidin-bead capture.

For the initial SPPLAT, 1 ml lysate from $2x10^6$ SPPLATed cells was added to 100 μl slurry of high-capacity Neutravidin resin (Thermo Fisher Scientific, Inc.), incubated with end-over-end rotation for 1 h at 4˚C, washed three times with lysis buffer containing sodium thiocyanate to reduce non-specific interactions, then biotinylated proteins were eluted with lysis buffer containing 10 mM biotin. Eluted proteins were separated by SDS-PAGE (10%) and stained with Simply Blue™ SafeStain Coomassie (Invitrogen; Thermo Fisher Scientific, Inc.) for 1 h at room temperature prior to dividing and excising equally into 16 bands. Gel slices were de-stained in ddH_2O and 20 mM NH_4HCO_3, reduced with 2 mM DTT and alkylated with 10 mM iodoacetamide prior to overnight digestion with 2 μg sequencing grade trypsin (Promega Corporation). Peptides were extracted with acetonitrile and 1% formic acid and re-suspended in water with 1% formic acid after vacuum-drying.

For SILAC SPPLAT, 5 ml cell lysates were quantified and equal amounts (1 mg) of protein from both heavy and light cell lysates were added to 0.5 ml slurry of high-capacity Neutravidin resin and incubated as mentioned above. Reciprocal labelling (specific-light, control-heavy) and affinity purification was also performed. Two rounds of 200 μl eluted proteins were combined and precipitated with 80% ice cold acetone, re-suspended in 1X SDS sample buffer and separated by SDS-PAGE (10%) as before, but were separated for only 1 cm; 4 bands per lane were excised for mass spectrometry (MS) analysis and prepared as before.

Identification of proteins and biotinylated proteins by MS. All liquid chromatography (LC)-MS/MS SPPLAT experiments were performed using a NanoAcquity UPLC system (Waters Corp.) and an LTQ Orbitrap Velos hybrid ion trap mass spectrometer (Thermo Fisher Scientific, Inc.). Separation of peptides was performed by reverse-phase chromatography using a Waters reverse-phase nano column (BEH C18, 75 μm i.d. x250 mm, 1.7 μm particle size) at a flow rate of 300 nl/min. Peptides were initially loaded onto a pre-column (Waters UPLC Trap Symmetry C18, 180 μm i.d. x20 mm, 5 μm particle size) from the NanoAcquity sample manager with 0.1% formic acid for 3 min at a flow rate of 10 μl/min. After this period, the column valve was switched to allow the elution of peptides from the pre-column onto the analytical column, where a linear gradient of increasing acetonitrile (5-35%) over 60 min was employed. The LC eluant was sprayed into the mass spectrometer by means of a nanospray source. All m/z values of eluting ions were measured in the Orbitrap Lumos Velos mass analyser, set at a resolution of 30,000. Data-dependent scans (top 10) were employed to automatically isolate and generate fragment ions by collision-induced dissociation in the linear ion trap, resulting in the generation of MS/MS spectra. Ions with charge states of ≥2+ were selected for fragmentation. The raw MS data files were converted to mgf files and searched against the Swissprot Human database (accessed in May 2017; 71,567 entries) using the Mascot search algorithm (version 2.3.02, Matrix Science) with methionine oxidation (M) as a variable modification and cysteine carbamidomethylation (C) as a fixed modification, allowing 2 missed cleavages, a peptide mass tolerance of ±1 Da and a fragment mass tolerance of 0.8 Da. Single-peptide hits were removed from the lists.

Quantitation was performed using MaxQuant (version 1.6.0.1; https://www.maxquant.org/). Raw data were searched using Andromeda (http://www.coxdocs.org/doku.php?id=maxquant:andromeda), with Arg-6 and Lys-6 set as heavy labels, methionine oxidation and N-acetylation as variable modifications, and cysteine carbamidomethylation as a fixed modification. The proteins were identified if there was at least one unique peptide and quantified if there were at least two unique peptides. Only unique peptides were used for quantitation.

Identification of the SK-BR-3 proteome by MS. SK-BR-3 cells ($1x10^5$) were grown in either McCoy's medium or RPMI-1640 and lysed, and the soluble fraction was separated by 10% SDS-PAGE, Coomassie-stained as described above, and the entire lane was excised to allow the analysis of all proteins by MS. The stained bands were reduced and alkylated, and MS was performed as described above.

Co-localisation of B7-H4 with its molecular neighbours. To confirm the co-localisation of B7-H4 with integrins, HLA-E or plexin, SK-BR-3 cells (~$1x10^4$) were spun onto 13 mm coverslips, fixed, but not permeabilised, washed, blocked and incubated with goat anti-B7-H4 polyclonal IgG Ab (1:250; cat. no. PA5-47261; Thermo Fisher Scientific, Inc.), and then either integrin α1 (mouse anti-human IgG_1 at 2 μg/ml; cat. no. MAB1973; EMD Millipore), HLA-E (mouse anti-human IgG_1 at 1:50; cat. no. sc-71262; Santa Cruz Biotechnology, Inc.) or plexin B2 (mouse anti-human IgM at 1:50; cat. no. sc-373969; Santa Cruz Biotechnology, Inc.) for 1 h at room temperature. Integrin α1 incubations were also performed at 4 and 37˚C. Incubations with anti-goat IgG-488 (1:1,000; cat. no. A-11078; Thermo Fisher Scientific, Inc.) and anti-mouse IgG-647 (1:1,000; cat. no. A-21239; Thermo Fisher Scientific, Inc.) for 1 h at room temperature were performed to visualise the cell surface proteins using confocal microscopy, as mentioned before.

Proximity ligation assay (PLA). SK-BR-3 cells (~$1x10^4$) were spun onto coverslips pre-coated with 0.05% poly L-lysine. Live cells were washed and blocked in 10% BSA in PBS and incubated with goat anti-B7-H4 (2.5 μg/10^6 cells) in 10% BSA for 30 min at room temperature to induce clustering, then fixed with 4% paraformaldehyde at room temperature for 10 min and washed in PBS. For controls, cells were first incubated in antibodies against integrin α1 (2 μg/ml; cat. no. MAB1973; EMD Millipore), HLA-E (1:50; cat. no. sc-373969; Santa Cruz Biotechnology, Inc.) or plexin B2 (1:50; cat. no. sc-373969; Santa Cruz Biotechnology, Inc.) for 1 h at room temperature. Controls included fixing cells prior to B7-H4 antibody incubation and omission of the primary antibodies. Sigma PLA probes (goat plus and mouse minus; Sigma Aldrich; Merck KGaA) were used and the ligation and amplification (far red) was performed according to the manufacturer's instructions. Cells on coverslips were mounted onto slides and imaged

using an Olympus Fluoview IX81 laser scanning confocal microscope (Olympus Corporation) at x60 magnification.

Real-time integrin binding. SK-BR-3 cells were seeded at $1x10^4$ cells/well in an E-plate (Roche Applied Science) pre-coated with either 10 μg/ml fibronectin or 10 μg/ml collagen peptides or 5% albumin. The wells were incubated with 20 μg/ml human anti-B7-H4 (MedImmune), or non-specific human IgG (1:100 dilution of ascitic fluid; in-house; MedImmune). To quantitate cell-line binding to collagen peptides, the impedance-based xCELLigence system (Acea), which allows label-free, dynamic monitoring of cell adhesion in real time, was used (23). The assay system expresses the adhesion-dependent rise in well impedance in units of cell index (CI), defined as $(R_n-R_b)/15$, where R_n is the electrical impedance of each cell-containing well and R_b is the background impedance of the well with medium alone. CI was measured for up to 2 h. All experiments were performed in triplicate in the presence of either 5 mM Mg^{2+} or 5 mM EDTA. Data are presented as the mean ± standard deviation and were analysed for statistical significance using one-way ANOVA followed by Tukey's post hoc test using the GraphPad Prism software package (version 7.0d, GraphPad Software, Inc.).

PCR of integrin isoforms. Total RNA was extracted from ~$5x10^6$ SK-BR-3 cells using an RNA extraction kit (Qiagen GmbH). RT-PCR was carried out with 1 mg of RNA, using the One-Step RT-PCR kit (Qiagen GmbH), following the manufacturer's instructions. The amplification primers used were as follows: Human integrin α1, forward 5'-GGTGAATCATTA CCTTGCGT-3' and reverse 5'-AGCACATCTCCAGAAGAA GC-3'; human integrin β1, forward 5'-AGGAACAGCAGA GAAGCTCA-3' and reverse 5'-CATTTTCTTCAATTTTCC CC-3'.

Co-immunoprecipitation (co-IP). To confirm direct binding of α1 integrin and surface B7-H4, antibodies to α1 integrin (EMD Millipore) and B7-H4 (MedImmune) were coupled to separate preparations of Protein G beads (Thermo Fisher Scientific, Inc.) overnight at 4˚C with gentle agitation. To assess only surface interactions of α1 integrin, IP was performed with live cells, as lysates would contain predominantly cytosolic B7-H4. Live cells ($1x10^6$) were washed in PBS and allowed to bind antibody-bound Protein G beads. Control cells were first incubated in goat serum with a non-specific antibody, and then Protein G beads were added. Unbound beads were washed off and cells were then lysed in lysis buffer as before. Soluble lysates were separated by SDS-PAGE (10%), transferred to a nitrocellulose membrane and probed with either antibodies to α1 integrin (1:3,000; EMD Millipore) or B7-H4 (1:2,000; Thermo Fisher Scientific, Inc.) for the B7-H4 and α1 integrin co-IP, respectively.

Results

Analysing the SK-BR-3 proteome. A partial SK-BR-3 proteome was obtained, which enables estimation of the abundance of common proteins that may also reside in the footprint of the SPPLAT biotin label and thus specifically bind affinity resins. For a stringent list, single-peptide hit protein assignments were removed, enabling positive identification of 1,220 proteins that were ranked by empirical abundance using the protein EMPAI score (Table SI). These equated to ~0.77% coverage of the expected total human proteome (currently 159,552 protein entries) and were interpreted with caution if they appeared in SPPLAT downstream purifications. Gene Ontology (GO) annotation analysis identified no over- or under-representation of any 'cell components' compared with the human reference proteome, indicating successful solubilisation and extraction of all protein classes. These abundant proteins included keratins, histones, metabolic enzymes, structural and heat shock proteins. The target protein, B7-H4, was not identified as a high-abundance protein, as expected, thereby highlighting the fact that a method for specifically labelling these B7 cell surface membrane proteins is required to identify proximal proteins.

This analysis also compared SK-BR-3 cells grown in McCoy's medium and the RPMI-1640 medium required for SILAC labelling. There was a large (86%) overlap in identified peptides for the most abundant proteins from each condition, indicating that the culture of SK-BR-3 cells in RPMI-1640 medium for quantitative analysis would not result in a significant change in the proteome.

The plasma membrane B7-H4 microenvironment. The localisation of B7-H4 in SK-BR-3 cells was first characterised and its weak plasma membrane expression compared with abundant intracellular expression was confirmed (Fig. 1A-C), suggesting its suitability for investigation via the SPPLAT method. Analysing B7-H4 3D structures using PDB structures identified B7-H4 only having two surface exposed tyrosine residues that are required for SPPLAT labelling. Confocal imaging and western blotting confirmed that B7-H4 and its neighbours were biotinylated (Fig. 1D and E). As a comparison, targeting B7-H1 resulted in biotinylation of a different, and smaller, set of proteins to B7-H4, as determined by western blotting (Fig. 1E). The negative control, using an HRP-tagged non-specific IgG, did not lead to biotinylation of any proteins.

This non-quantitative B7-H4 SPPLAT experiment followed by affinity purification (AP)-MS resulted in the identification of 2,004 biotinylated proteins (Table SII). The B7-H4 protein and its proximal proteins were enriched and identified, a number of which were not identified in the initial SK-BR-3 proteome screen. GO annotation revealed an enrichment of cell surface and peripheral membrane proteins compared with the control, as expected. The top 80 cell surface-associated proteins from the anti-B7-H4 SPPLAT experiment that include the target, VTCN1 (B7-H4), ICOS ligand (B7-H2), a number of integrins, plexins, cell adhesion molecules and proteins from the Ig superfamily are shown in Table I. A number of cytosolic proteins were also identified, suggesting that the biotin-tyramide can permeate the plasma membrane in the 5-min labelling time and/or that cytosolic proteins can be recruited to the plasma membrane upon B7-H4 activation by antibody. As a further comparison, B7-H1 was also labelled (Fig. 1E), and several immune signalling molecules were identified, a number of which were also associated with B7-H4 (Table SI), although the protein microenvironments differed. The negative control did not non-specifically label signalling molecules.

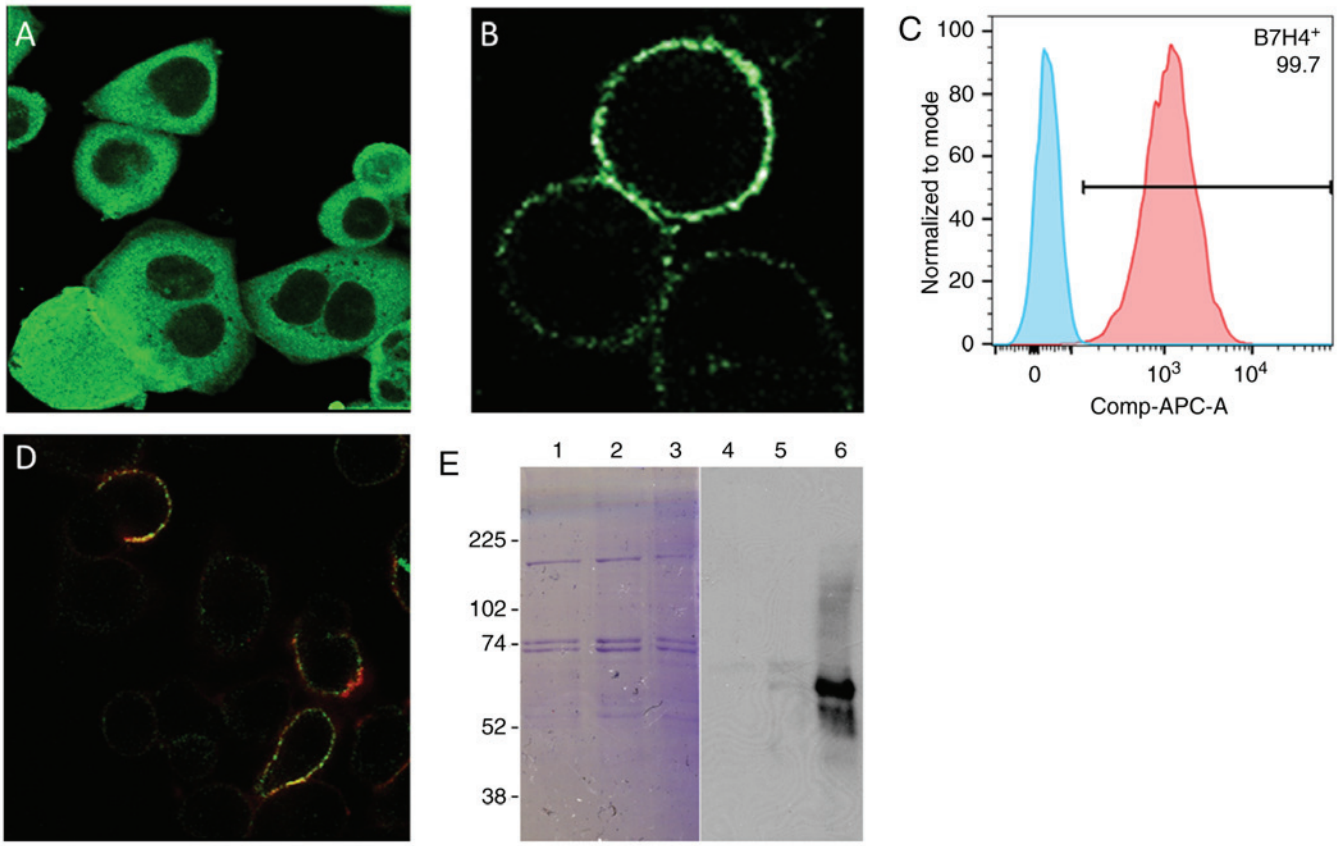

Figure 1. B7-H4 presence (A) in permeabilised SK-BR-3 cells and (B) on the cell surface of SK-BR-3 cells. (C) Flow cytometry analysis of SK-BR-3 cells where blue represents non-specific antibody (isotype control) and pink is anti-B7-H4 to confirm plasma membrane association, (D) the co-localisation of B7-H4 and biotin after SPPLAT, and (E) Coomassie-staining of proteins eluted from neutravidin beads (lanes 1-3) and streptavidin-HRP blot to confirm biotinylation of eluted proteins (lanes 4-6). Lanes 1 and 4, SPPLAT labelling with HRP-tagged non-specific IgG, lanes 2 and 5, SPPLAT labelling with HRP-tagged anti-B7-H1, lanes 3 and 6, SPPLAT labelling with HRP-tagged anti-B7-H4. Images are representative from 3 replicate experiments. SPPLAT, specific proteomic proximity labelling assay using tyramide; HRP, horseradish peroxidase.

In order to quantify the enrichment of proteins in an anti-B7-H4-SPPLAT experiment compared with a negative control IgG, a SILAC SPPLAT analysis was performed, where cells cultured in isotope-labelled media were labelled via SPPLAT for 2 min to minimise membrane diffusion and cytosolic labelling. In performing two biological replicates and two reciprocal labellings, 938 proteins were identified, of which 452 were present in all four datasets (Table SIII). By performing control experiments with a non-specific IgG, a significant proportion (~90%) of proteins that demonstrated minimal expression changes between the anti-B7-H4 and non-specific IgG control were eliminated. Subsequently, the 13 proteins that demonstrated a log2 fold-change of >2 and significance of P>0.01 (log10 adjusted P-value of 2) between the test and control experiments were analysed; in addition to plasma membrane-localised proteins, there were some cytoplasmic and nuclear proteins, despite a short labelling time (Fig. 2). One identified plasma membrane protein, Enox1, an Ecto-NOX disulphide-thiol exchanger, is involved in electron transport to the cell surface and has not previously been reported to be associated with B7-H family members. A total of 13 predicted binding partners of Enox1 were not found in our list, notably Protein GREB1, which is considered to play a role in oestrogen-stimulated cell proliferation by acting as a regulator of hormone-dependent cancer growth in breast and prostate cancers. A cytosolic candidate, interleukin enhancer-binding factor 3, interacts with and inhibits viral mRNAs (24); therefore, it was not further investigated. The remainder of increased fold changed proteins were metabolic or nucleus-localised and were also not further investigated. As B7-H4 was exclusively SPPLATed and not detected in the SILAC SPPLAT, the present study focused on the proteins that were present only in the B7-H4 labellings and absent in controls with relevant GO annotation, good peptide coverage and abundance, as indicated by EmPAI scoring or peak intensity from MaxQuant analysis (listed in Table I). Of particular interest were several integrins, HLA-E and plexins. These were further investigated using PLA, CoIP and binding studies.

Validation of B7-H4 proximal proteins by PLA. The SPPLAT method can biotinylate proteins within a 100-nm footprint of the target HRP-coupled antibody-ligand interaction. PLA can validate our identified proteins and further positions within 40 nm. PLA was performed on integrin α1, HLA-E and plexin B2. As shown in Fig. 3, when SK-BR-3 cells are pre-incubated with B7-H4 antibody, this induces B7-H4 clustering at the cell surface, and both integrin α1 and HLA-E co-localise with B7-H4 forming distinct clusters compared to when no B7-H4 antibody incubation occurs (Fig. 3A-E).

Table I. Proteins from replicate SPPLAT experiments.

Uniprot identifier	Gene symbol	Protein description	EMPAI score	Fold enrichment	No. Peptides	% sequence coverage
A8K6Q8	TFRC	cDNA FLJ75881, highly similar to H. sapiens transferrin receptor (p90, CD71) (TFRC), mRNA	6.11	2.01	48	51.7
A5YM53	***ITGAV***	***Integrin α-5***	***2.27***	***7.09***	***44***	***37.2***
A0A087WXM8	BCAM	Basal cell adhesion molecule	1.99		20	43.0
B7Z9S8	ATP1B1	Sodium/potassium-transporting ATPase subunit β	1.97		8	37.2
O15031	***PLXNB2***	***Plexin-B2***	***1.84***	***4.97***	***60***	***35.2***
D3DVF0	F11R	F11 receptor, isoform CRA_a	1.64	3.49	10	29.3
P05026	ATP1B1	Sodium/potassium-transporting ATPase subunit β-1	1.45	2.59	8	28.0
O75054	IGSF3	Immunoglobulin superfamily member 3	1.19	3.31	34	31.4
P14384	CPM	Carboxypeptidase M	1.12	4.00	12	28.6
Q969P0-3	IGSF8	Isoform 3 of immunoglobulin superfamily member 8	1.09		12	28.3
P01860	IGHG3	Immunoglobulin heavy constant gamma 3 (G3m marker)	0.97	12.13	9	21.4
B4DDZ4	ANXA4	Annexin	0.92		8	27.0
H0YIC4	CS	Citrate synthase	0.91		3	24.3
B2R6C4	REEP5	Receptor expression-enhancing protein	0.8	2.35	3	10.2
O43570-2	CA12	Isoform 2 of carbonic anhydrase 12	0.78		7	24.1
Q5U0H8	MPZL1	Myelin protein zero-like 1	0.71		4	15.9
Q2TTR7	EGFR	Receptor protein-tyrosine kinase	0.67		23	21.3
A0A0A8LFF7	***HLA-E***	***MHC class I antigen***	***0.66***		***2***	***20.1***
Q5T2L0	**VTCN1**	**V-set domain-containing T-cell activation inhibitor 1**	**0.65**		**5**	**18.5**
Q6N093	IGHG2	Putative uncharacterized protein DKFZp686I04196	0.61		7	20.1
Q16625-3	OCLN	Isoform 3 of occludin	0.6		9	25.0
Q8WTV0-2	SCARB1	Isoform 1 of scavenger receptor class B member 1	0.56	4.67	7	15.9
A4D1S0	KLRG2	Killer cell lectin-like receptor subfamily G member 2	0.55		6	16.8
P18084	ITGB5	Integrin β-5	0.53		12	16.0
Q14126	DSG2	Desmoglein-2	0.52	3.06	16	17.6
P10586-2	PTPRF	Isoform 2 of receptor-type tyrosine-protein phosphatase F	0.51	6.38	31	21.8
Q7Z7H5-2	TMED4	Isoform 2 of transmembrane emp24 domain-containing protein 4	0.47		3	13.2
P05556	***ITGB1***	***Integrin β-1***	***0.42***	***3.82***	***11***	***16.2***
Q7Z3Z9	L1CAM	L1 cell adhesion molecule	0.41	3.42	19	16.4
P17301	ITGA2	Integrin α-2	0.41	2.16	16	14.9
F8VY02	ERP29	Endoplasmic reticulum resident protein 29	0.41		2	10.6
Q9UEI6	PVRL2	Polio virus-related protein 2, α isoform	0.39	2.79	5	12.9
B4DW34	SMPDL3B	cDNA FLJ56798, highly similar to acid sphingomyelinase-like phosphodies terase 3b	0.37	2.85	5	12.0
B4DL19	ANXA1	Annexin	0.37		2	9.8
A0A087WUV8	BSG	Basigin	0.35		2	14.8
A0A0A0MSA9	PVR	Poliovirus receptor	0.34	4.25	4	14.2

Table I. Continued.

Uniprot identifier	Gene symbol	Protein description	EMPAI score	Fold enrichment	No. Peptides	% sequence coverage
O00622	CYR61	Protein CYR61	0.34		4	10.8
O75144	***ICOSLG***	***ICOS ligand***	***0.32***		***3***	***10.2***
B4DU18	CDH5	cDNA FLJ51093, highly similar to Cadherin-5	0.31	7.75	8	12.5
F5GXJ9	ALCAM	CD166 antigen	0.31	6.20	6	13.3
Q9BS26	ERP44	Endoplasmic reticulum resident protein 44	0.31	2.21	4	11.0
Q969N2-5	PIGT	Isoform 5 of GPI transamidase component PIG-T	0.31		5	8.4
B1AP13	CD55	Complement decay-accelerating factor	0.29		4	7.4
A8K6K4	IL1RAP	cDNA FLJ77565, highly similar to H. sapiens interleukin 1 receptor accessory protein (IL1RAP)	0.27		5	7.5
B1AMW1	CD58	CD58 antigen, (lymphocyte function-associated antigen 3), isoform CRA_c	0.26		2	7.5
Q9UNN8	PROCR	Endothelial protein C receptor	0.26		2	9.2
B4DPN0	APOH	cDNA FLJ51265, moderately similar to β-2-glycoprotein 1 (β-2-glycoprotein I)	0.22		2	5.4
G3V124	TMPRSS4	Transmembrane protease serine 4	0.18		2	8.9
A0A024R798	SLC44A2	Choline transporter-like protein 2 isoform 2	0.17	4.25	6	7.8
B3KP89	GNAO1	cDNA FLJ31446 fis, highly similar to Guanine nucleotide-binding protein G(o) subunit α 1	0.17		2	6.4
Q5TG12	PTPRK	Receptor-type tyrosine-protein phosphatase κ	0.17		8	6.7
D6RBJ7	GC	Vitamin D-binding protein	0.17		2	8.6
B4DDE5	SLC5A6	cDNA FLJ56614, highly similar to sodium-dependent multivitamin transporter	0.15	2.14	3	10.0
P06727	APOA4	Apolipoprotein A-IV	0.15		2	4.5
P36955	SERPINF1	Pigment epithelium-derived factor	0.15		2	6.4
Q13641	TPBG	Trophoblast glycoprotein	0.15		2	5.0
B2RAF9	ST14	Suppressor of tumorigenicity 14 protein homolog	0.14		4	5.6
Q6EMK4	VASN	Vasorin	0.14		4	7.8
Q96GQ5	C16orf58	RUS1 family protein C16orf58	0.13	2.17	2	7.6
Q9Y5L3-2	ENTPD2	Isoform short of ectonucleoside triphosphate diphosphohydrolase 2	0.13		2	4.6
Q53G72	BCAP31	B-cell receptor-associated protein 31 variant	0.12		2	8.1
B4DTS6	CD97	cDNA FLJ54117, highly similar to CD97 antigen	0.12		3	5.1
Q9Y490	TLN1	Talin-1	0.1	2.00	11	4.0
A0A087WVP1	FAT1	Protocadherin Fat 1	0.1		20	4.5
S4R3V8	LSR	Lipolysis-stimulated lipoprotein receptor	0.1		2	4.3
P29317	EPHA2	Ephrin type-A receptor 2	0.09		3	2.4
B4E0H8	ITGA3	cDNA FLJ60385, highly similar to integrin α-3	0.09		3	2.7
B4DTY8	***ITGA1***	***cDNA FLJ61587, highly similar to Integrin α-1***	***0.08***		***3***	***1.8***

Table I. Continued.

Uniprot identifier	Gene symbol	Protein description	EMPAI score	Fold enrichment	No. Peptides	% sequence coverage
Q5R3F8	ELFN2	Protein phosphatase 1 regulatory subunit 29	0.07		2	1.7
B2RBY8	ENPP1	FLJ95771, highly similar to *H. sapiens* ectonucleotide pyrophosphatase/ phosphodiesterase 1 (ENPP1)	0.07		2	1.9
P05543	SERPINA7	thyroxine-binding globulin	0.07		2	4.0
H0Y858	n/a	Uncharacterized protein IL1 r binding	0.07		3	4.3
Q08345-5	DDR1	Isoform 4 of epithelial discoidin domain-containing receptor 1	0.06		3	3.1
O14678	ABCD4	ATP-binding cassette sub-family d member 4	0.05		3	2.1
Q9UIW2	PLXNA1	Plexin-A1	0.05		3	1.5
A0A024R9Q1	THBS1	Thrombospondin 1, isoform CRA_a	0.05		2	1.9
Q04721	NOTCH2	Neurogenic locus notch homolog protein 2	0.04		3	1.4
B2R7F8	PLG	Plasminogen	0.04		2	1.8
Q9UHN6	TMEM2	Transmembrane protein 2	0.04		3	1.3
Q9Y4D7	PLXND1	Plexin-D1	0.03		2	0.9

Cell surface and membrane proteins from two replicate non-quantitative and SILAC SPPLAT experiments that were absent in control labelling, ranked by mean EmPAI score. Underlined text indicates the presence of B7-H1 control in non-quantitative experiments. Bold print indicates the 'bait' proteins. Proteins in bold italics were of interest and were further validated. Full list is provided in Table SII. EMPAI, empirical abundance index, fold enrichment over proteins also discovered in B7H1 SPPLAT; SPPLAT, specific proteomic proximity labelling assay using tyramide; SILAC, table isotope labelling of amino acids in culture.

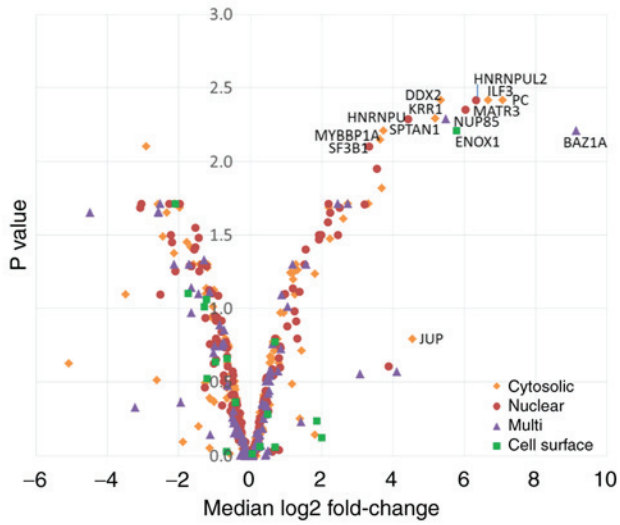

Figure 2. Distribution of quantified proteins from two biological and two reciprocal labelled SILAC SPPLAT experiments (n=4). Data are categorised by Gene Ontology cell component. SPPLAT, specific proteomic proximity labelling assay using tyramide; SILAC, stable isotope labelling of amino acids in culture.

Plexin B2 was not found to co-localise with B7-H4 at the cell surface (Fig. 3F and G); however, standard immunofluorescence demonstrated co-localisation just beneath the plasma membrane (Fig. 3H).

Functional studies show that integrin α1 associates with B7-H4. Several integrin subunits (α1, α2, α3, αV, β1 and β5) were identified in the B7-H4 SPPLAT AP-MS screen. Integrins function as αβ heterodimers in various combinations, and several, such as αV and β5, have been implicated in tumour growth, so were used as positive controls in validation experiments. Integrin α1 operates in partnership with β1 and β5. The PLA experiment demonstrated that integrin α1 was indeed within 40 nm of B7-H4 on the plasma membrane (Fig. 3A) and, in parallel, it was confirmed by RT-PCR that α1 and β1 are expressed in SK-BR-3 cells (Fig. 4A). To assess whether α1 and β1 interact with B7-H4 on the cell surface, integrin real-time binding assays were performed with known substrates of integrin heterodimers α1β1 (collagen receptor) and α5β1 (fibronectin receptor) in the presence and absence of anti-B7-H4 (blocking) antibody. The presence of B7-H4 in close proximity to integrins α1 and β1 could modulate integrin-substrate binding and, furthermore, the presence of a blocking antibody for B7-H4 may alter binding. Indeed, the presence of anti-B7-H4 reduced binding of SK-BR-3 cells, via α1, to collagen substrates at 0.5 h (Fig. 4B), whereas the cell binding response to fibronectin was significantly higher ($P<0.0001$) in the presence of an anti-B7-H4.

To ensure that integrins were not being non-specifically activated due to the PLA being performed at 37˚C, antibody incubation at 4˚C was also performed prior to fixation; no differences in the expression or internalisation were observed

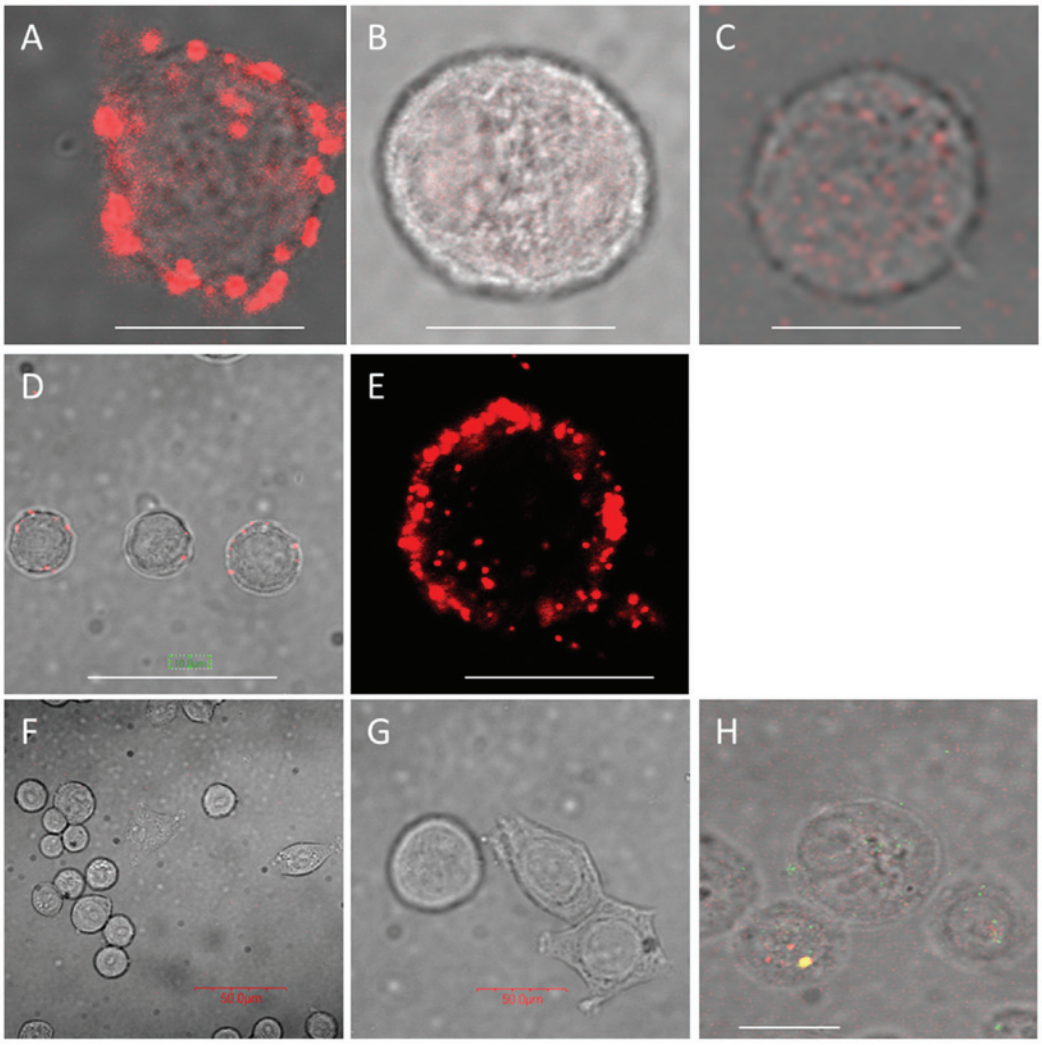

Figure 3. Proximity ligation assay (PLA) was employed to confirm proximity of enriched proteins (A-C) integrin α1, (D and E) HLA-E and (F-H) plexin B2. (A) SK-BR-3 cells were pre-incubated with anti-B7-H4 to induce clustering showing proximal integrin α1; (B) prefixed cells showing no surface integrin α1. (C) No B7-H4 antibody negative control (background). (D) Cells pre-incubated with anti-B7-H4 showing co-localised HLA-E; (E) cells not pre-incubated with anti-B7-H4 showing disperse HLA-E. (F) Cells pre-incubated with B7-H4 showing plexin B2 not co-localising with B7-H4 on the cell surface. (G) Cells with anti-B7-H4 only (negative control). (H) Plexin B2 (red) co-localising (yellow) with B7-H4 (green) intracellularly following permeabilization. All images are bright field with red overlay, except E. Scale bars: 10 μm, unless otherwise indicated. Images are representative from 3 replicate experiments.

(Fig. S2A-D). To assess whether integrin α1 is a direct binding partner of B7-H4, co-IP was performed in SK-BR-3 cells using an antibody to B7-H4 to pull down B7-H4-bound proteins, and subsequent detection of integrin α1 by western blotting (Fig. S2E). The anti-B7-H4 pulled down integrins, whilst a control anti-B7-H4 Fab alone did not pull down B7-H4 with integrins α1 and β1, thus confirming that integrin α1 is in a complex with B7-H4 (Fig. S2E). Thus, multiple lines of evidence show that integrin α1 is found in a complex with B7-H4 on the cell surface.

HLA-E was another interesting find, as its role is typically in negative regulation of the immune system. Its close proximity to B7-H4 confirmed by SPPLAT and PLA (Fig. 3D and E) was further validated by co-IP and found to be in complex with B7-H4 at the cell surface (Fig. S2F).

Only a limited number of SPPLAT hits that had both high and low scoring EMPAI values were investigated. There were also several Ig superfamily members and antigens, such as CD58/LFA-3, ALCAM and L1CAM, EGFR and ST14 in the B7-H4 microenvironment that may play a role that would warrant further validation.

Discussion

The role of B7-H4 in tumorigenesis is unclear. In order to gain an insight into the function of B7-H4, the human breast cancer cell-line SK-BR-3 was used to identify proteins closely located in the cell membrane. SPPLAT is a useful tool for surveying protein environments on the cell surface, especially low abundance proteins such as the B7 family. The specific targeting of membrane proteins by SPPLAT, using antibodies in this case, facilitates their identification and characterisation. However, understanding highly abundant proteins is crucial for carefully designing such targeted experiments in order to minimise false positives especially as upon cell lysis, all proteins mix and may vary in concentration of 100 orders of magnitude. These include cytosolic carboxylases, which bind streptavidin affinity resins in our downstream

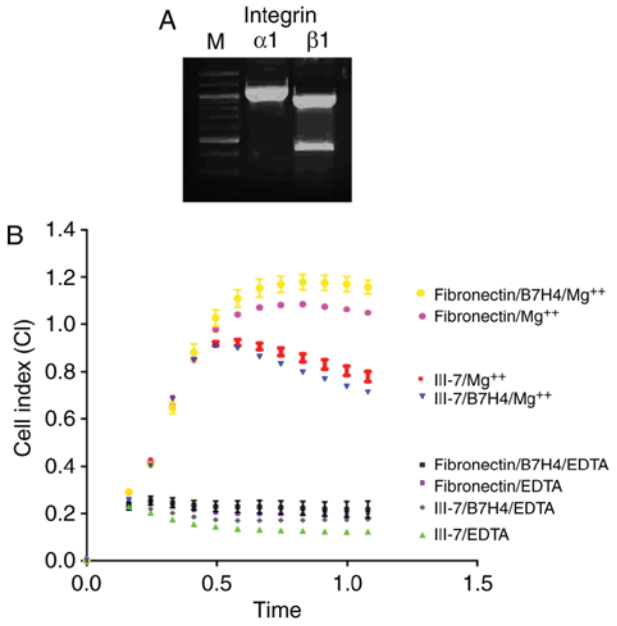

Figure 4. (A) Quantitative PCR was performed to confirm the presence of integrins α1 and β1 in SK-BR-3 cells. (B) Real-time integrin binding study in SK-BR-3 cells in the presence and absence of B7-H4 antibody. Fibronectin was used as the substrate for the integrin α5 and β1 complex, and III7 (a GLOGEN peptide that recognises collagen III) was used as the substrate for the integrin α1 and β1 complex. The presence of EDTA acts as a control, as it blocks the metal ion-dependent adhesion site in all integrin molecules. Experiments were performed three times, each in triplicate, and a representative is shown with mean values. A one-way ANOVA with Tukey's post hoc test was performed for each real-time and end-point for each replicate. Binding of fibronectin in presence of B7-H4 antibody was significant ($P<0.0001$) compared with no antibody or with EDTA controls. Binding of collagen in the presence of B7-H4 antibody was not significantly different.

purification steps. Therefore, a partial SK-BR-3 proteome was obtained, which enables estimation of the abundance of common proteins that may also reside in the footprint of the biotin label and thus specifically bind affinity resins. These may often dominate low-abundance cell surface proteins that are more difficult to extract and characterise, which are the focus of the present study. Thus far, few proteomic analyses of SK-BR-3 cells have been reported comparing proteins to a normal human mammary epithelial cell line (25), both of which used 2D-DIGE, which is inefficient at resolving membrane proteins. Thus, a more comprehensive list of the more abundant proteins was also presented in the present study. The aim was not to characterise the entire proteome, but rather to be aware of the top 1% of abundant proteins, as these may bind non-specifically to proteins that have been labelled for identifying surface microenvironments. No over- or under-representation of Protein Groups was observed, and abundant proteins were mostly structural proteins.

B7-H4 has previously been reported to interact with only a handful of proteins, mainly involved in adaptive immunity. Using SPPLAT, another family member of B7-H4, B7-H2 (ICOSL), and a number of novel interacting and proximal proteins within a 100-nm radius on the surface of SK-BR-3 cells were identified. The only experimentally reported interactor of B7-H4 is a *trans* interactor, BTLA, a B- and T-lymphocyte attenuator, a lymphocyte inhibitory receptor that inhibits lymphocytes during immune response and unlikely to reside on APCs. Our SPPLAT method did not identify any of the three reported B7-H4 co-expressing interacting proteins described by STRING, namely IL6 (an activator of B7-H4), CD80 or CTLA4 found on T-cells. Other putative interactors predicted by literature text mining, such as PDCD1LG2, a programmed cell death 1 ligand 2, involved in the costimulatory signal and essential for T-cell proliferation and IFNG production in a PDCD1-independent manner, IL4, CD28 and CD86, were not identified. These were all low-scoring STRING predictions. However, other programmed cell death proteins, PDCD5 and PDCD6, were identified in its interacting protein PDCD6IP. By contrast, a whole new family of proteins were identified in the B7-H4 microenvironment, namely integrins. These candidates were further narrowed down to within 40 nm. and co-IP was used to confirm direct interaction. Previous reports have suggested roles for integrin subunits in tumour development. The present study investigated α1β1, as there has been no previous report of this heterodimer being associated with B7-H4. Its substrate is collagen, and its function is to mediate collagen synthesis. It has been reported than integrin α1β1 mediates a unique collagen-dependent proliferation pathway *in vivo* in pancreatic cancer cells (26), and this may also be the case in breast cancer cells. Our confirmation of the presence of integrin α1β1 by RT-PCR, immunofluorescence and proximity to B7-H4 by PLA and direct binding by xCELLigence cell binding assays and co-IP suggest that these two integrin subunits function as a α1β1 heterodimer and mediate a collagen-dependent proliferation pathway *in vivo* in breast cancer cells akin to pancreatic cells mentioned previously.

Several integrin subunits were found in our SPPLAT screen, a number of which form functional heterodimers: α1β1, α2β1, α3β1, α5β1, αVβ1 and α1β5. Integrins are transmembrane adhesion receptors that provide the physical link between the actin cytoskeleton and the extracellular matrix. It has been well established that integrins play a major role in various cancer stages, such as tumour growth, progression, invasion, metastasis and angiogenesis. In breast cancer, integrin αV-β3 has been associated with high malignant potential in cancer cells, signalling the onset of widespread metastasis. Expression of αV integrins and identification of the vitronectin receptor have been reported in breast cancer cells (27). Other reports have confirmed α5β1 integrin as a pertinent therapeutic target (28). Integrins α3 and α2, both independently dimerising with β1, were also identified in the SPPLAT experiment along with their interacting partners, basigin and talin, confirming the presence of multiple integrin subunits and macromolecular complexes at the cell surface. Whilst reports suggest overexpression of combinations of different integrin subunits in a variety of cancers, it was not identified as an abundant family of proteins from SK-BR-3 lysates in our partial proteome study.

The present study also identified other interacting proteins, including HLA-E, a key regulator of both the innate and adaptive immune response through positive regulation of several interleukins, such as IL4 and IL13, and interferon signalling (29). In addition, the present study identified several plexins, some of which have been implicated in cancer. One of these, PLXNA4 in complex with SemA3 and neuropilin-1 has been reported to be the receptor of B7-H4 on regulatory

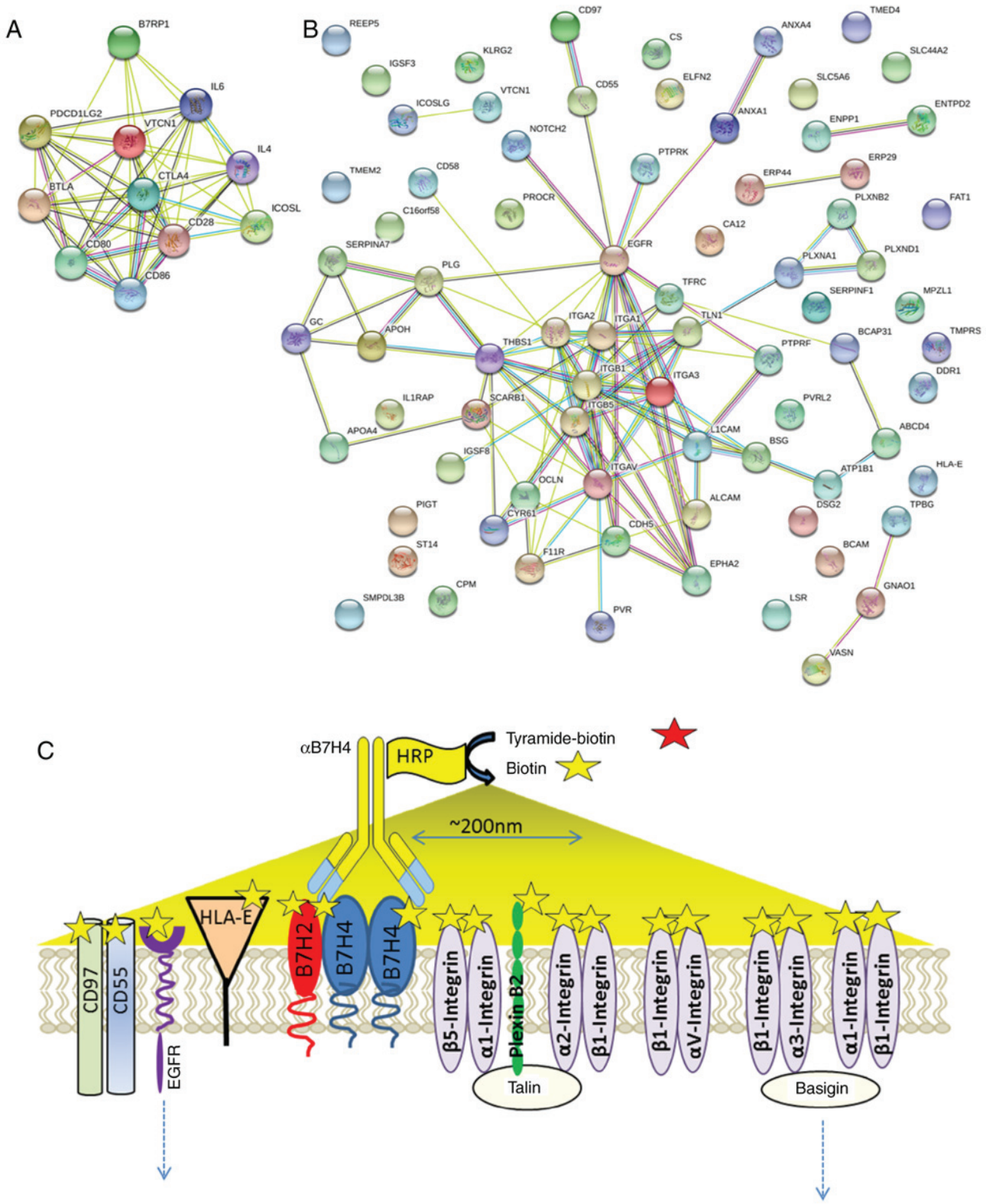

Figure 5. (A) Known interactors of B7-H4 using STRING. (B) Novel proteins proximal to B7-H4 using STRING. (C) A snapshot of the B7-H4 cell surface microenvironment. STRING, Search Tool for the Retrieval of Interacting Genes/Proteins.

CD4 T-cells (30). Another plexin identified as being in close proximity to B7-H4 on the cell surface, PLXNB2, is required for the physiological and pathological functions of angiogenin (ANG) and has significant therapeutic potential in solid and hematopoietic cancers and neurodegenerative diseases (31). In addition, quantitative SILAC demonstrated increased expression of Enox1 that has previously been implicated in immune regulation: As a candidate gene for the autoimmune disease myasthenia gravis (32), and as a biomarker of response to an anti-IL6 mAb in rheumatoid arthritis (33).

It appears the B7-H4 surface microenvironment in SK-BR-3 cells is complex upon binding anti-B7-H4, whereby

an assortment of proteins are recruited to the cell surface upon induced clustering by the HRP-labelled antibody. The data were screened using the STRING programme, which compares our data with experimental and computationally predicted interactors (Fig. 5A and B) and a model was proposed based on known and newly identified associate proteins (Fig. 5C). Little overlap of the predicted (Fig. 5A) and our findings (Fig. 5B) was observed. Clearly, integrins are highly connected and, the plexin cluster is associated with the integrins via talin. In fact, 54% of the proteins were connected, suggesting a complex process in signalling. HLA-E appears to be unconnected along with the B7 family, so this is a novel finding.

SPPLAT is a useful tool for identifying membrane interacting proteins. This technique may work in several ways. First, one can identify proteins proximal to a selected target by using an antibody, drug or toxin coupled to HRP that can aid delivery of biotin-tyramide to a region of ~100 nm. Second, one can identify new receptors or ligands on the cell surface by similarly HRP-labelling a selected ligand or receptor and SPPLATing the cell surface to identify the unknown receptor or ligand, respectively.

Acknowledgements

We would like to thank Richard Farndale for his helpful discussions.

Funding

JSR and APJ were funded by BBSRC H024085/1 and AstraZeneca. LC and SWH were funded by the Department of Biochemistry, University of Cambridge.

Availability of data and material

The datasets used and/or analysed during the current study are available from the corresponding author on reasonable request.

Authors' contributions

JSR performed the majority of the experiments. LCCC performed the experiments presented in Fig. 1. SWH performed the reverse transcription-PCR and xCELLigence assay. GD performed flow cytometry experiments. JSR and APJ wrote the manuscript with helpful comments from AS, GD and NT. NT, AS, GD, JSR, KSL and APJ conceived and designed the project and helped analyse and interpret the results.

Ethics approval and consent to participate

Not applicable.

Patient consent for publication

Not applicable.

Competing interests

JSR and APJ were funded by AstraZeneca; GD, AS and NT are employees of AstraZeneca.

References

1. Huppa JB and Davis MM: The interdisciplinary science of T-cell recognition. Adv Immunol 119: 1-50, 2013.
2. Schildberg FA, Klein SR, Freeman GJ and Sharpe AH: Coinhibitory pathways in the B7-CD28 ligand-receptor family. Immunity 44: 955-972, 2016.
3. Chen L and Flies DB: Molecular mechanisms of T cell co-stimulation and co-inhibition. Nat Rev Immunol 13: 227-242, 2013.
4. Keir ME, Butte MJ, Freeman GJ and Sharpe AH: PD-1 and its ligands in tolerance and immunity. Annu Rev Immunol 26: 677-704, 2008.
5. Salomon B and Bluestone JA: Complexities of CD28/B7: CTLA-4 costimulatory pathways in autoimmunity and transplantation. Annu Rev Immunol 19: 225-252, 2001.
6. Sica GL, Choi IH, Zhu G, Tamada K, Wang SD, Tamura H, Chapoval AI, Flies DB, Bajorath J and Chen L: B7-H4, a molecule of the B7 family, negatively regulates T cell immunity. Immunity 18: 849-861, 2003.
7. Prasad DV, Richards S, Mai XM and Dong C: B7S1, a novel B7 family member that negatively regulates T cell activation. Immunity 18: 863-873, 2003.
8. Salceda S, Tang T, Kmet M, Munteanu A, Ghosh M, Macina R, Liu W, Pilkington G and Papkoff J: The immunomodulatory protein B7-H4 is overexpressed in breast and ovarian cancers and promotes epithelial cell transformation. Exp Cell Res 306: 128-141, 2005.
9. Afreen S and Dermime S: The immunoinhibitory B7-H1 molecule as a potential target in cancer: Killing many birds with one stone. Hematol Oncol Stem Cell Ther 7: 1-17, 2014.
10. Tringler B, Zhuo S, Pilkington G, Torkko KC, Singh M, Lucia MS, Heinz DE, Papkoff J and Shroyer KR: B7-h4 is highly expressed in ductal and lobular breast cancer. Clin Cancer Res 11: 1842-1848, 2005.
11. Xie N, Cai JB, Zhang L, Zhang PF, Shen YH, Yang X, Lu JC, Gao DM, Kang Q, Liu LX, *et al*: Upregulation of B7-H4 promotes tumor progression of intrahepatic cholangiocarcinoma. Cell Death Dis 8: 3205, 2017.
12. Abadi YM, Jeon H, Ohaegbulam KC, Scandiuzzi L, Ghosh K, Hofmeyer KA, Lee JS, Ray A, Gravekamp C and Zang X: Host b7x promotes pulmonary metastasis of breast cancer. J Immunol 190: 3806-3814, 2013.
13. Huang H, Li C and Ren G: Clinical significance of the B7-H4 as a novel prognostic marker in breast cancer. Gene 623: 24-28, 2017.
14. Franchina DG, He F and Brenner D: Survival of the fittest: Cancer challenges T cell metabolism. Cancer Lett 412: 216-223, 2018.
15. Ni L and Dong C: New B7 family checkpoints in human cancers. Mol Cancer Ther 16: 1203-1211, 2017.
16. Pardoll DM: The blockade of immune checkpoints in cancer immunotherapy. Nat Rev Cancer 12: 252-264, 2012.
17. Podojil JR and Miller SD: Potential targeting of B7-H4 for the treatment of cancer. Immunol Rev 276: 40-51, 2017.
18. Vogt AB, Spindeldreher S and Kropshofer H: Clustering of MHC-peptide complexes prior to their engagement in the immunological synapse: Lipid raft and tetraspan microdomains. Immunol Rev 189: 136-151, 2002.
19. Rees JS, Li XW, Perrett S, Lilley KS and Jackson AP: Protein neighbors and proximity proteomics. Mol Cell Proteomics 14: 2848-2856, 2015.
20. Li XW, Rees JS, Xue P, Zhang H, Hamaia SW, Sanderson B, Funk PE, Farndale RW, Lilley KS, Perrett S and Jackson AP: New insights into the DT40 B cell receptor cluster using a proteomic proximity labeling assay. J Biol Chem 289: 14434-14447, 2014.
21. Rees JS, Li XW, Perrett S, Lilley KS and Jackson AP: Selective proteomic proximity labeling assay using tyramide (SPPLAT): A quantitative method for the proteomic analysis of localized membrane-bound protein clusters. Curr Protoc Protein Sci 88: 19.27.1-19.27.18, 2017.
22. Neve RM, Chin K, Fridlyand J, Yeh J, Baehner FL, Fevr T, Clark L, Bayani N, Coppe JP, Tong F, *et al*: A collection of breast cancer cell lines for the study of functionally distinct cancer subtypes. Cancer Cell 10: 515-527, 2006.
23. Hamaia SW, Pugh N, Raynal N, Némoz B, Stone R, Gullberg D, Bihan D and Farndale RW: Mapping of potent and specific binding motifs, GLOGEN and GVOGEA, for integrin alpha-1beta1 using collagen toolkits II and III. J Biol Chem 287: 26019-26028, 2012.
24. Li X, Liu CX, Xue W, Zhang Y, Jiang S, Yin QF, Wei J, Yao RW, Yang L and Chen LL: Coordinated circRNA biogenesis and function with NF90/NF110 in viral infection. Mol Cell 67: 214-227.e7, 2017.

25. Ziegler YS, Moresco JJ, Tu PG, Yates JR III and Nardulli AM: Plasma membrane proteomics of human breast cancer cell lines identifies potential targets for breast cancer diagnosis and treatment. PLoS One 9: e102341, 2014.
26. Pozzi A, Wary KK, Giancotti FG and Gardner HA: Integrin alpha1beta1 mediates a unique collagen-dependent proliferation pathway in vivo. J Cell Biol 142: 587-594, 1998.
27. Meyer T, Marshall JF and Hart IR: Expression of alphav integrins and vitronectin receptor identity in breast cancer cells. Br J Cancer 77: 530-536, 1998.
28. Schaffner F, Ray AM and Dontenwill M: Integrin alpha5beta1, the fibronectin receptor, as a pertinent therapeutic target in solid tumors. Cancers (Basel) 5: 27-47, 2013.
29. Rieger L, Hofmeister V, Probe C, Dietl J, Weiss EH, Steck T and Kämmerer U: Th1- and Th2-like cytokine production by first trimester decidual large granular lymphocytes is influenced by HLA-G and HLA-E. Mol Hum Reprod 8: 255-261, 2002.
30. Podojil JR, Chiang MY, Ifergan I, Copeland R, Liu LN, Maloveste S, Langermann S, Liebenson D, Balabanov R, Chi H, *et al*: B7-H4 modulates regulatory CD4$^+$ T cell induction and function via ligation of a semaphorin 3a/Plexin A4/Neuropilin-1 complex. J Immunol 201: 897-907, 2018.
31. Yu W, Goncalves KA, Li S, Kishikawa H, Sun G, Yang H, Vanli N, Wu Y, Jiang Y, Hu MG, *et al*: Plexin-B2 mediates physiologic and pathologic functions of angiogenin. Cell 171: 849-864.e25, 2017.
32. Landouré G, Knight MA, Stanescu H, Taye AA, Shi Y, Diallo O, Johnson JO, Hernandez D, Traynor BJ, Biesecker LG, *et al*: A candidate gene for autoimmune myasthenia gravis. Neurology 79: 342-347, 2012.
33. Maldonado-Montoro M, Cañadas-Garre M, González-Utrilla A, Plaza-Plaza JC and Calleja-Hernández MẎ: Genetic and clinical biomarkers of tocilizumab response in patients with rheumatoid arthritis. Pharmacol Res 111: 264-271, 2016.